

QM/MM Simulation of the Hydrogen Bond Dynamics of an Adenine:Uracil Base Pair in Solution. Geometric Correlations and Infrared Spectrum

Yun-an Yan and Oliver Kühn*

Institut für Physik, Universität Rostock, D-18051 Rostock, Germany

(Dated: November 2, 2018)

Abstract

Hybrid QM(DFT)/MM molecular dynamics simulations have been carried out for the Watson-Crick base pair of 9-ethyl-8-phenyladenine and 1-cyclohexyluracil in deuteriochloroform solution at room temperature. Trajectories are analyzed putting special attention to the geometric correlations of the N-H \cdots N and N-H \cdots O hydrogen bonds in the base pair. Further, based on empirical correlations between the hydrogen bond bond length and the fundamental NH stretching frequency its fluctuations are obtained along the trajectory. Using the time dependent frequencies the infrared lineshape is determined assuming the validity of a second order cumulant expansion. The deviations for the fundamental transition frequencies are calculated to amount to less than 2% as compared with experiment. The width of the spectrum for the N-H \cdots N bond is in reasonable agreement with experiment while that for the N-H \cdots O case is underestimated by the present model. Comparing the performance of different pseudopotentials it is found that the Troullier-Martins pseudopotential with a 70 Ry cut-off yields the best agreement.

PACS numbers: 71.15.Pd, 82.30.Rs, 82.39.Pj, 87.16.dt, 87.64.km

*Electronic address: oliver.kuehn@uni-rostock.de

I. INTRODUCTION

One of the primary examples for the importance of hydrogen bonding is its role in the structural selectivity of the pairing of nucleic acid bases in DNA [1]. Here double and triple hydrogen bonds (HBs) are formed whose theoretical characterization still poses a challenge as it combines many features of multidimensional condensed phase quantum dynamics. Infrared (IR) spectra are particularly sensitive to HB formation. The broad lineshapes not only contain information on the intramolecular couplings, but the underlying fluctuation dynamics also reflects the interaction with the surrounding medium [2, 3]. The spectroscopic signatures of hydrogen bonding in heterodimers of various bases have been investigated in different phases. Isolated adenine:thymine pairs, for instance, were studied in gas phase using IR-UV double resonance experiments [4]. This provided evidence that Watson-Crick pairing does not result in the most probable form under these conditions. Later, the dominant tautomer could be identified on the basis of quantum dynamical simulations of IR spectra including anharmonicity [5]. Ultrafast nonlinear IR spectroscopy has been used to scrutinize the vibrational dynamics of individual base pairs in solution [6]. Here it was found, for instance, that the life time of the H-bonded NH stretching fundamental transition decreased by a factor of three as compared to the monomer case, thus demonstrating the effect of HB mediated anharmonic couplings. The next step in complexity has been addressed by ultrafast two-color IR studies of the HBs in DNA oligomers. Heyne et al. showed that excitation in the fingerprint region provides, by virtue of the anharmonic couplings, a means to identify, for instance, the symmetric NH₂ stretching vibration of adenine:thymine pairs upon probing in the 3200 cm⁻¹ range [7]. In the linear IR spectrum this range is completely masked by the absorption of water molecules. Subsequently, the assignment has been confirmed by anisotropy measurements [8].

Since first principles quantum dynamical simulation of condensed phase HB dynamics will remain elusive different approximate strategies are usually followed. In order to capture the electronic structure associated with H-bonding density functional theory (DFT) seems to be most appropriate as long as stacking interactions are of minor importance [9]. By running classical trajectories with on-the-fly DFT forces the IR spectrum can be obtained from the Fourier transform of the dipole autocorrelation function. Of course, this completely neglects quantum effects in the nuclear motion. The latter are frequently accounted for by quantum correction factors [10]. Car-Parrinello molecular dynamics

(CPMD) has proven to be particularly well-suited for simulating condensed phase dynamics including H-bonded systems. A pioneering contribution has been given by Silvestrelli et al. who determined the IR spectrum of liquid water [11]. Subsequent applications to aqueous solutions, e.g., of uracil have been summarized in Ref. [12]. More recent studies focussed on strongly H-bonded system like the Zundel cation in the crystalline phase [13].

In principle quantum effects for the fast proton stretching motion can be recovered by calculating its potential energy curve for selected configurations along the CPMD trajectory (snapshot potentials). Upon solving the stationary Schrödinger equation for these potentials one obtains a set of fundamental transition frequencies. The combination of CPMD and snapshot potentials for the proton stretching motion has been put forward in Ref. [14]. In this reference an intramolecular N-H \cdots O HB in a Mannich base in gas and crystalline phase was considered. The IR spectrum has been calculated by convolution of the stick spectrum obtained along the trajectory with a Gaussian. This gave a band maximum below 2000 cm⁻¹, considerably red shifted with respect to the estimated experimental value. Interestingly, the analogous simulation in CCl₄ solution gave a band whose first moment has been well above 2000 cm⁻¹, pointing out the sensitivity with respect to the environment [15]. In Ref. [16] the method was applied to an *N*-oxide which exhibits two rather strong nonequivalent O-H \cdots O HBs in the unit cell. Here, two-dimensional snapshot potentials including the bending vibration of the HB had been considered as well. Finally, a different *N*-oxide in the crystalline phase with a rather strong HB was studied in Ref. [17]. In this case a 1000 cm⁻¹ broad distribution of transition frequencies for the OH-stretching fundamental was found from one-dimensional snapshot potentials in reasonable agreement with experiment.

Quantum Mechanics/Molecular Mechanics (QM/MM) hybrid methods have been developed to cope with situations where only a part of a large system needs to be treated at the quantum mechanical level (for a review, see Ref. [18]). Here the crucial point is the interface between the QM and MM parts and in the context of CPMD different schemes for the most delicate issue of the nonbonding electrostatic interactions have been developed [19, 20]. A series of impressive applications to the IR spectroscopy of various forms of water clusters in a model of bacteriorhodopsin has been presented in Refs. [21, 22, 23].

Recently, we have applied the QM/MM approach to the determination of the IR line-shape of the uracil NH stretching vibration in a modified adenine:uracil (A:U) pair in deuteriochloroform solution [24]. In doing so we made use of an empirical NH-frequency-N \cdots N-distance correlation which gave access to the fluctuating transition frequency along

the trajectory (see also Ref. [25]). From the autocorrelation function of this transition frequency the lineshape could be determined. This procedure gave the band maximum at 3209 cm^{-1} and the full-width at half maximum (FWHM) of 39 cm^{-1} , both values being in reasonable agreement with experiment [6].

In the present contribution we will extend our previous study in several respects. First, the IR spectral features of both intermolecular HBs are investigated. This requires to establish a distance-frequency correlation for N-H \cdots O HBs which is done on the basis of available crystal structure data. Alternatively, we explore the possibility to use snapshot potentials for obtaining this correlation curve. It will turn out that the snapshot frequencies underestimate the average transition frequency considerably and are of little use for the considered intermolecular HBs. In order to scrutinize this issue we report an investigation of the influence on the used pseudopotential (PP) and kinetic energy cut-off parameter in the DFT calculation. Besides the IR spectrum we will put emphasis on the geometric correlations across the double HBs which can be obtained along the trajectory. This concerns in particular the linearity, planarity, and the correlation between HB distance and proton position.

The paper is organized as follows: In the next Section II we start by defining the model system and the QM/MM protocol. Further, the issues of geometric correlations and lineshape analysis are discussed. In Section III we first give results on geometric correlations before we come to the lineshape and its dependence on the PP used. The results are summarized in Section IV.

II. METHODS

A. QM/MM Protocol

We will investigate the vibrational dynamics of 9-ethyl-8-phenyladenine (A) and 1-cyclohexyluracil (U) solvated in CDCl_3 which has been studied experimentally by Woutersen and Cristalli [6]. To this end a hybrid QM/MM method is used as implemented in the Gromacs/CPMD interface [20]. All atoms of the A:U pair except those belonging to the substituents are dealt with quantum mechanically by the CPMD package [26]. The substituents themselves as well as the solvent are described by the OPLS all-atom force field [27] as implemented in Gromacs [28]. H-atom capping is used to saturate the dangling bonds at the QM/MM boundary (see Fig. 1). In the simulation a single A:U pair is

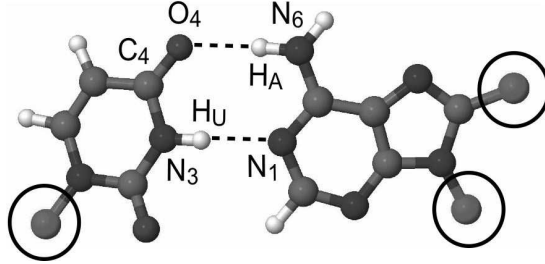


FIG. 1: QM part of the A:U base pair with the capping atoms indicated by circles. In the analysis below we will use the angles α (N_6 - O_4 - C_4) and β (C_4 - N_3 - N_1), the angle γ between the two vectors $\vec{N_3N_1}$ and $\vec{O_4N_6}$ as well the dihedral angle ϕ defined by the atoms N_1 , N_3 , O_4 , and N_6 .

solvated in 100 CDCl_3 molecules within a box having dimensions $30.0 \text{ \AA} \times 23.5 \text{ \AA} \times 23.5 \text{ \AA}$ (density is 0.1 M [6]). The QM part is placed in a $21.2 \text{ \AA} \times 15.9 \text{ \AA} \times 15.9 \text{ \AA}$ box. The Becke exchange and Lee-Yang-Par correlation functional (BLYP) together with the plane wave basis set is used as implemented in the CPMD code. The MM molecular dynamics run is performed at 298 K using a time step of 2 fs. Note that in the current Gromacs/CPMD implementation it is actually a Born-Oppenheimer simulation which is performed. For the initial configuration the geometry of the optimized gas phase base pair replacing solvent atoms in the equilibrated simulation box has been used. First, a 1 ps equilibration run was performed using the Vanderbilt (VB) ultrasoft PP with a plane wave cutoff of 30 Ry. Subsequently, trajectories were propagated up to 5.0 ps using different PPs and cut-off parameters, i.e., VB [29] with a cut-off of 30 Ry and 40 Ry, Troullier-Martins (TM) PP [30] with 70 Ry and 100 Ry, and Goedecker (GO) PP [31] with 100 Ry and 140 Ry. Except for the comparative studies the results presented are based on the TM PP using a cut-off of 70 Ry.

B. Hydrogen Bond Geometry

Hydrogen bonds $\text{A-H} \cdots \text{B}$ display remarkable correlations in their geometry. Limbach and coworkers promoted a model which gives a simple explanation of these correlation in terms of valence bond orders p_i viewing the HB as composed of two diatomic units A-H and B-H with bond lengths R_1 and R_2 , respectively [32]:

$$p_i = \exp\{-(R_i - R_i^{\text{eq}})/b_i\}, \quad (1)$$

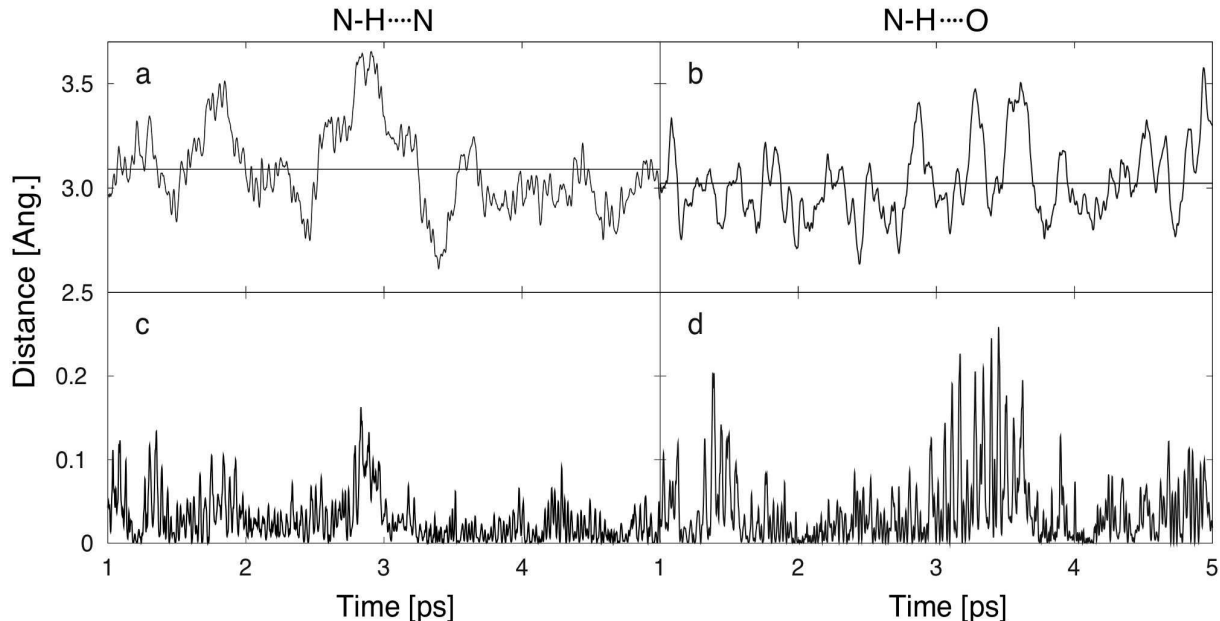


FIG. 2: Geometric parameters of the HBs along the trajectory: (a) and (b) HB lengths of N-H \cdots N and N-H \cdots O, respectively. The horizontal line indicates the time average. (c) and (d) out-of-line motion of the H atom in the two HBs, measured by the difference $L(\text{N-H}) + L(\text{N}\cdots\text{H}) - L(\text{N}\cdots\text{N})$ and $L(\text{N-H}) + L(\text{O}\cdots\text{H}) - L(\text{N}\cdots\text{O})$, respectively.

where R_i^{eq} is the equilibrium bond length of the hypothetical nonbonded diatomic and b_i is a parameter describing the change of the bond valence upon bond stretching. If one assumes that the total bond order is unity, i.e. $p_1 + p_2 = 1$, the two bond lengths cannot be changed independently. This can be alternatively expressed in terms of the deviation from the HB center $(R_1 - R_2)/2$ and the HB length $R_1 + R_2$. The correlation curve so obtained from numerous structural data expresses a fact well known from quantum chemical studies of potential energy surfaces, namely that the HB is compressed upon H transfer while passing the transition state [2]. This correlation for a given type of HB - although expressed in Eq. (1) by four parameters only - yields a rather robust description of the HB geometries (see, e.g. the case of N-H \cdots N bonds in Refs. [32, 33]). It turns out, however, that in particular for short HBs the original formulation required some modification. In Ref. [34] Limbach et al. suggested an empirical correction as follows

$$p_{1/2}^{\text{H}} = p_{1/2}^{\text{H}} \mp c(p_1 - p_2)(p_1 p_2)^5 - d(p_1 p_2)^2, \quad (2)$$

for which $p_1^{\text{H}} + p_2^{\text{H}} < 1$ holds. Here, c and d are parameters to be determined by fitting geometric correlations to experimental data.

The change in the potential energy surface which is reflected in the above geometric

correlation also manifests itself in a dependence of the AH stretching frequency on the HB length. In a seminal work Novak collected experimental data on different H-bonded crystals to establish A-B bond length-frequency correlation for N-H \cdots N and O-H \cdots O bonds [35]. Later, this study was extended to asymmetric HBs by Mikenda [36]. For the case of N-H \cdots N bonds the correlation has been expressed previously by the function [24]

$$f(r) = \omega_\infty/2\pi c \operatorname{erf} \left(\sum_{i=0}^2 a_i r^i \right), \quad (3)$$

where ω_∞ is the free NH stretching frequency in gas phase (for parameters see caption of Fig. 6). Eq.(3) can also be used for asymmetric HBs such as those of N-H \cdots O type involving also HBs formed by amine groups (see Supplementary Information). The advantage of such relation is obvious, it allows to assign stretching frequencies along a trajectory on the basis of atomic coordinates only [24].

C. IR Lineshape

In the classical limit the IR lineshape can be calculated straightforwardly from the trajectory by means of the dipole-dipole correlation function [45]. Here we will use lineshape theory and account for the quantum nature of the high-frequency proton stretching vibrations. Specifically, we will calculate their gap correlation function, defined for some fundamental stretching frequency, $\omega_{10}(t)$, along a trajectory as follows:

$$C(t) = \langle (\omega_{10}(t) - \langle \omega_{10} \rangle) (\omega_{10}(0) - \langle \omega_{10} \rangle) \rangle, \quad (4)$$

where $\langle \omega_{10} \rangle$ denotes the mean value along the trajectory. Assuming a second order cumulant expansion to hold the IR spectrum can be expressed via the lineshape function

$$g(t) \equiv \int_0^t d\tau \int_0^\tau d\tau' C(\tau'), \quad (5)$$

as [37]

$$\sigma(\omega) = \frac{1}{\pi} \operatorname{Re} \int_0^\infty dt e^{i(\omega - \langle \omega_{10} \rangle)t - g(t)}. \quad (6)$$

Of course, Eq. (4), is a classical quantity and does not satisfy detailed balance. There are various recipes to compensate for this deficiency by introducing quantum correction factors [10]. Recently, Skinner and coworker gave an interesting account on this issue which revealed that for the exemplary case of HOD in D₂O quantum corrections have a only modest influence on the IR lineshape [38]. In order to take into account quantum

effects we will fit the classical correlation function to the expression obtained within the multimode oscillator model [37]

$$C(t) = \sum_j S(\omega_j) \omega_j^2 \coth(\hbar\omega_j/2k_B T) \cos(\omega_j t) + i \sum_j S(\omega_j) \omega_j^2 \sin(\omega_j t), \quad (7)$$

where $S(\omega_j)$ is the dimensionless Huang-Rhys factor giving the coupling strength between the two-level system and the bath mode with frequency ω_j . These two sets of parameters are used for fitting the real part of $C(t)$ obtained from the classical molecular dynamics which in turn gives the imaginary part as well.

III. RESULTS

A. Geometry-based Correlations

In Fig. 2a and 2b we depict the N \cdots N and the N \cdots O distance, respectively, along the production part of the trajectory. In the course of the trajectory no H-atom transfer occurs. The average HB lengths are $L(\text{N}\cdots\text{N}) = 3.09 \text{ \AA}$ and $L(\text{N}\cdots\text{O}) = 3.03 \text{ \AA}$. Since geometry-based correlations are usually discussed assuming linear HBs we illustrate in panels (c) and (d) of Fig. 2 the deviation of the H atoms from linear motion. The average deviations are 0.028 \AA for the N-H \cdots N and 0.038 \AA for the N-H \cdots O bond, that is, both cases can be considered to correspond to almost linear HBs.

The planarity of the gas phase A:U heterocycles is no longer present in solution. Focussing on the two HBs only, one can define the dihedral angle ϕ formed by the atoms N_1 , N_3 , O_4 , and N_6 (see. Fig. 1). Its average value during the propagation interval is -19° . Fig. 3 shows how this deformation is related to other geometrical changes of the HBs. From panel (a) we see that nonplanarity comes along with a decrease of the angle $\alpha + \beta$, that is, with a compression of the HBs due to N_3H_U and/or C_4O_4 bending vibrations. Fig. 3b reveals an almost perfect linear correlation between the dihedral angle ϕ and the angle γ describing the directions of the two HBs. Besides the geometric correlation between two HBs, there also exists correlation for each HB separately. Fig. 4 gives a test of the empirical correlation between N-H and HB length derived from Eq. (2). As anticipated from the robustness of the correlation reported before [32, 33, 34], geometries along the trajectory are remarkably well described by this simple expression. This holds true, irrespective of the deviation from linearity and planarity mentioned above. Moreover, there

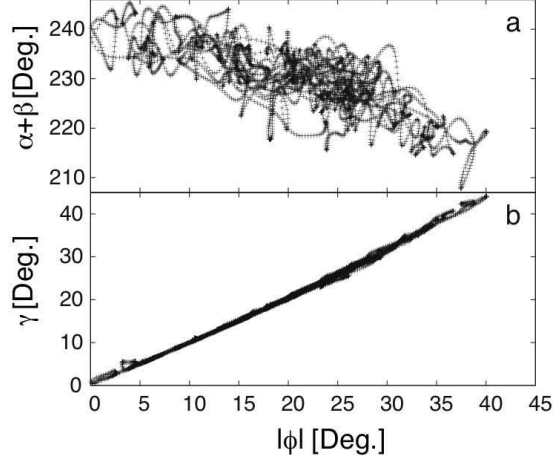


FIG. 3: Geometric correlations of the N-H \cdots N and N-H \cdots O HBs along the QM/MM trajectory between the absolute value of the dihedral angle ϕ and (a) the sum of the angles α and β and (b) the angle γ (for definitions see caption of Fig. 1).

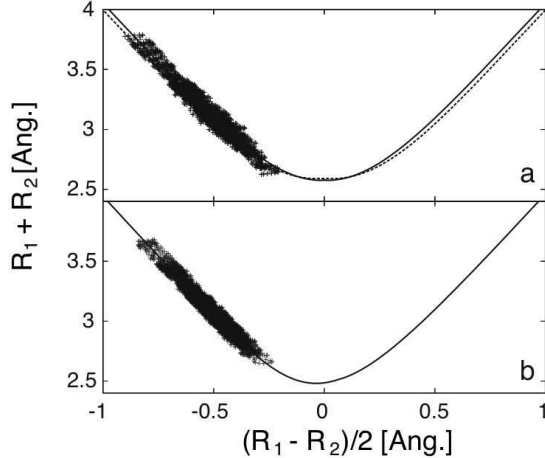


FIG. 4: Geometric correlations between HB length and H-atom position following from a fit to Eq. (2) (solid line) with the points sampled along the QM/MM trajectory. (a) N-H \cdots N ($1 = 2 = \text{NH}$) with $R_1^{\text{eq}} = 1.025 \text{ \AA}$, $b_1 = 0.361 \text{ \AA}$, $c = 577.64$, and $d = 0.30$ and (b) N-H \cdots O ($1 = \text{NH}$, $2 = \text{OH}$) with $R_1^{\text{eq}} = 1.021 \text{ \AA}$, $b_1 = 0.407 \text{ \AA}$, $R_2^{\text{eq}} = 1.029 \text{ \AA}$, $b_2 = 0.232 \text{ \AA}$, $c = 400$, $d = 0.21$. In panel (a) we also show the correlation curve from Limbach et al. (dashed line) [33].

seems to be little variance with respect to the class of molecules as shown by plotting the correlation curve with parameters obtained by Limbach et al. for intramolecular N-H \cdots N HBs (dashed line in panel (a)) [33].

In a next step we explore the correlation between HB bond lengths N \cdots N and N \cdots O and the fundamental transition frequencies of the NH stretching motion. A straightforward realization would consist in the calculation of NH stretching snapshot potentials in

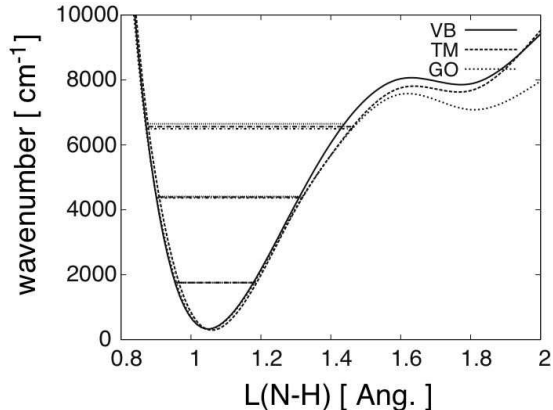


FIG. 5: Comparison of potential energy curves for the N-H \cdots N HB as calculated from different PPs by changing the N-H bond length (11 points in the given interval) with all other coordinates being fixed at the $t = 0$ ps structure. The horizontal lines correspond to the lowest vibrational states which have been obtained using the Fourier Grid Hamiltonian method [39]. The cut-off parameters are 30 Ry for VB, 70 Ry for TM and 140 Ry for GO.

an otherwise frozen geometry for some representative points along the trajectory. Interpolating these data one will have at hand a distance-frequency correlation to be used for all points along the trajectory. Fig. 5 depicts a representative potential for the N-H \cdots N HB and its dependence on the form of the PP. First, we notice that up to the overtone excitation the potential is rather well described by an anharmonic oscillator and the second rather shallow minimum corresponding to an H transfer configuration is energetically not favorable. Second, apart from the shape of this shallow transfer minimum the three PPs give rather similar fundamental transition frequencies, which are 2634 cm^{-1} for VB, 2647 cm^{-1} for TM and 2600 for GO. Third, the fundamental transition frequency in the 2600 cm^{-1} range is considerable lower than the experimental value of 3185 cm^{-1} [6].

A more complete picture is obtained from Fig. 6a where we show results from snapshot frequency calculations with the VB, TM and GO PPs sampled along the trajectory. They reproduce the expected qualitative dependence on the HB length, but are red-shifted by about 450 cm^{-1} with respect to the empirical correlation curve obtained from crystal data. This holds irrespective of the PP and cut-off parameter.

The first question to be clarified concerns the experimental assignment in Ref. [6]. In fact the similar case of 9-ethyladenine and cyclohexyluracil in chloroform has been studied previously and it was found that self-association of U:U dimers occurs which would have an NH stretching absorption in the $3000\text{-}3200\text{ cm}^{-1}$ range as well. However, the association constant for U:U dimers is 15 times smaller than for A:U ones, so that

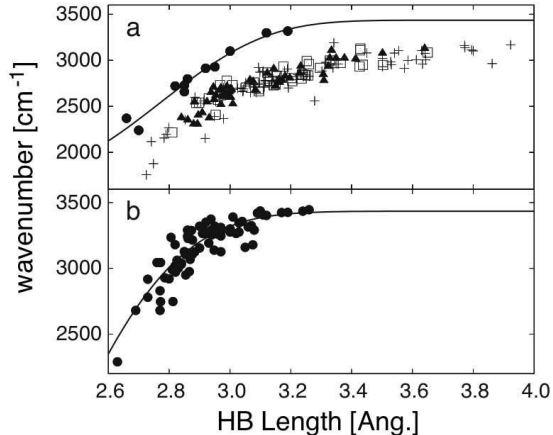


FIG. 6: (a) Correlation between HB length $N \cdots N$ and fundamental NH transition frequency (bullets: spectroscopic data for crystals containing intermolecular $N-H \cdots N$ HB [24, 35]; QM/MM on the fly frequencies using the VB (crosses), TM (squares), and GO (triangles) PPs with cut-off of 30 Ry, 70 Ry, and 140 Ry, respectively. The solid line is a fit of experimental data according to Eq. (3) with $\omega_\infty/2\pi c = 3436 \text{ cm}^{-1}$ [40], $a_0 = 7.0911$, $a_1 = -5.7941 \text{ \AA}^{-1}$, and $a_2 = 1.2711 \text{ \AA}^{-2}$. (b) Correlation between HB length $N \cdots O$ and fundamental N-H transition frequency (bullets: spectroscopic data for crystals containing intermolecular $N-H \cdots O$ HBs, solid line: fit according to Eq. (3) with $\omega_\infty/2\pi c = 3434 \text{ cm}^{-1}$ [40], $a_0 = -0.5345$, $a_1 = -0.8332 \text{ \AA}^{-1}$, and $a_2 = 0.5044 \text{ \AA}^{-2}$).

the contribution from U:U dimers should be negligible [41]. A similar conclusion can be reached based on the work of Miller et al. who demonstrated an 1:1 stoichiometry for similar purine and pyrimidine base analogues in CDCl_3 by monitoring the IR absorption changes around 3210 cm^{-1} as a function of the uracil mole fraction [42].

Giving this evidence for the correct experimental assignment, we compare the present findings with recent gas phase quantum chemical studies of the thymine NH stretching vibration in the adenine:thymine base pair [5]. In harmonic approximation the DFT/B3LYP (6-31++G(d,p)) level of theory yields a frequency of 2981 cm^{-1} . Accounting for anharmonicity within a three-dimensional model which includes all H-bonded stretching vibrations lowers this value to 2608 cm^{-1} . In order to rule out that this is a result of too soft DFT potential energy surfaces, MP2 corrections have been added to the diagonal anharmonicity. However, this causes an increase of the thymine stretching frequency to 2688 cm^{-1} only. Very recently, Yagi and coworkers have started to investigate this vibration using their VMP2-(4) method [43] on the basis of a B3LYP/6-31G++(d,p) full-dimensional quartic force field potential. They obtained a preliminary value as low as 2488 cm^{-1} [44].

At this level of theory the $\text{N}\cdots\text{N}$ distance is 2.88 \AA , which is smaller than the average value obtained from the QM/MM trajectory. Therefore, the lower value of the NH stretching frequency in the gas phase is consistent with the stronger HB as compared to the solution phase. However, giving the empirical correlations discussed in the following the absolute value of the calculated frequencies appears to be considerably too small.

To cope with this problem we decided to resort to an empirical mapping of HB distances to the stretching frequencies. In Ref. [24] we have shown that this correlation plotted in Fig. 6a gives an average frequency of 3227 cm^{-1} for the VB PP with a cut-off of 30 Ry and using a 6.2 ps trajectory. Furthermore, the lineshape derived from the frequency fluctuations has been in good agreement with the experiment as well. This supports the assumption that despite the discrepancy in the absolute value of the stretching frequency the current QM/MM protocol provides a reasonable description of the fluctuations influencing the HB. We have extended this approach to the case of the $\text{N-H}\cdots\text{O}$ bond; the frequency-HB length correlation plot derived from available crystal data is shown in Fig. 6b. Notice that the data used included HBs involving amine groups, that is, the fact that the considered vibrations is actually of symmetric NH_2 character is taken care of by the empirical relation. The resulting time-dependent frequencies for the two HBs are given in Fig. 7.

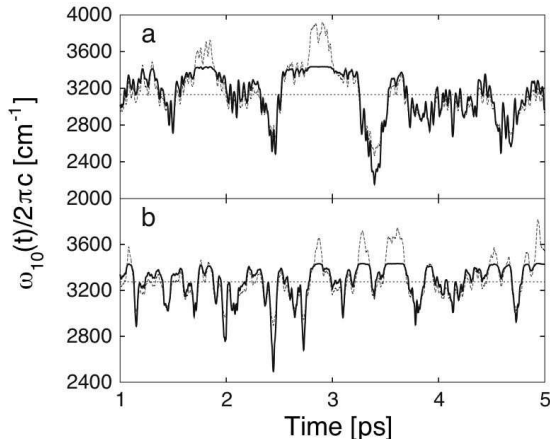


FIG. 7: Time-dependent fundamental transition frequencies for the $\text{N-H}\cdots\text{N}$ (a) and the $\text{N-H}\cdots\text{O}$ (b) HB as obtained using the empirical correlations displayed in Fig. 6. The dotted lines are the averaged values $\langle\omega_{10}\rangle$ which are equal to 3132 cm^{-1} in (a) and 3275 cm^{-1} in (b). The dashed lines are the $\text{N}\cdots\text{N}$ and $\text{N}\cdots\text{O}$ distances scaled and shifted such as to reveal the correlation with the time-dependent frequencies.

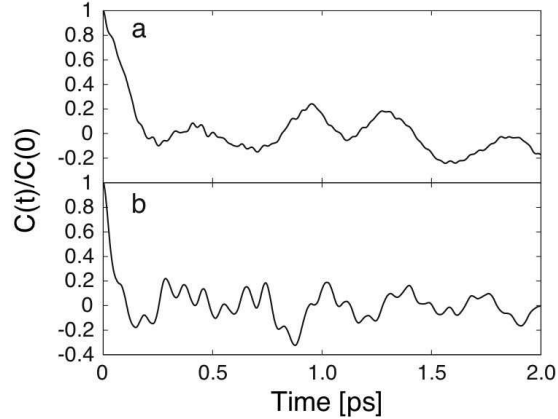


FIG. 8: Frequency correlation function, Eq. (4) for the NH stretching vibrations of (a) the N-H \cdots N and (b) the N-H \cdots O HB.

B. IR Lineshape Analysis

The correlation function $C(t)$ has been calculated for both HBs for the gap fluctuations shown in Fig. 7. The results given in Fig. 8 reveal a rapid initial decay followed by pronounced oscillations lasting up to the 2 ps which can be covered by the available trajectory (for a convergence study, see also Ref. [24]). In order to gain further insight into the distribution of modes coupled to the considered transitions, we have fitted $C(t)$ according to the Brownian oscillator model, Eq. (7). The chosen frequency range of 0-1770 cm^{-1} covers the low-frequency part of the calculated gas phase harmonic IR spectrum of the A:U pair. It is discretized into 20 modes whose frequencies and coupling strengths are used as fitting parameters. The distribution of coupling strengths $S(\omega)$ is shown in Fig. 9. First, we notice that both distributions are dominated by low-frequency vibrations. Second, in both cases we observe two smaller peaks which are around 200 and 500 cm^{-1} for N-H \cdots N as well as around 350 and 550 cm^{-1} for N-H \cdots O. It is tempting to assign these peaks to intermolecular vibrational modes. Indeed gas phase harmonic analysis of the A:U pair gives several intermolecular modes modulating the N \cdots N and N \cdots O distances in region of 150-400 cm^{-1} . Modes in the range of 400-600 cm^{-1} are mostly modulating the N \cdots O distance consistent with Fig. 9.

From the correlation functions one obtains the IR lineshape which is exemplarily shown for the N-H \cdots N case in Fig. 10. First we notice that the overall agreement with the experimental data is fairly good given the simple empirical model for assigning transition frequencies. In particular the asymmetry of the line is well reproduced. We also show the previous result obtained using the VB PP [24] which merely gives a slightly lower value

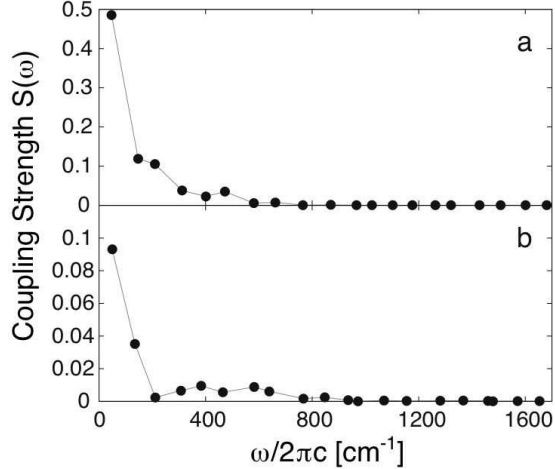


FIG. 9: Coupling strength between the NH vibration and the bath as function of the bath frequency. (a) results for N-H \cdots N HB; (b) results for N-H \cdots O HB. Points are fitted results and line is guide for eye.

for the FWHM.

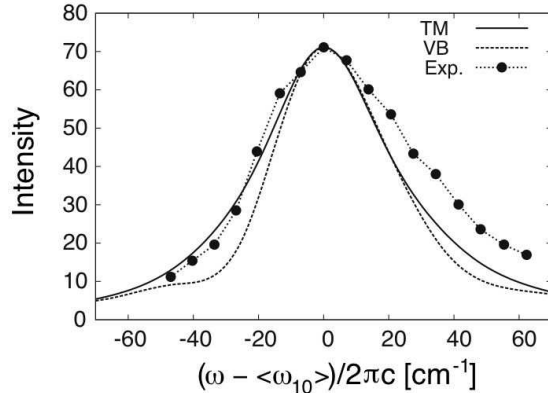


FIG. 10: IR lineshape of NH stretching compared with experimental data [6] (line for experimental result is drawn as guide for the eye only). Note that we have not included the shift of the transition frequency due to the imaginary part of the correlation function. It amounts to -3 cm^{-1} for the TM and -16 cm^{-1} for the VB case.

A detailed comparison of lineshape parameters obtained by using different PPs and cut-off parameters is presented in Tab. I. If we take the average transition frequencies and the corresponding energy gap between the two stretching vibrations as the measure for the performance of the method, we find that the TM PP with a cut-off of 70 Ry gives the best results. Here the deviations from experimental values are below 2 % for both frequencies. Of course, this result is not general in the sense that it is based on the proposed simulation protocol which includes the empirical mapping of distances to frequencies. Therefore

TABLE I: Comparison of HB geometry and lineposition and lineshape for different PPs and cut-off parameters. Labels $L_{N\dots N/O}$, $\nu_{NH\dots N/O}$ and $\Gamma_{N\dots N/O}$ stand for bond length, fundamental transition frequency and the FWHM of the IR lineshape for $NH\dots N/O$ HB, respectively. Gap refers to the distance between the fundamental transition frequency of $N-H\dots N$ and $N-H\dots O$ HBs and $\Gamma_{N\dots N}^{AI}$ to the FWHM of the $N-H\dots N$ HB based on the stretching-distance correlation from snapshot potentials. The TM (70 Ry) setup has been used in Fig. 10. Note that the frequencies do not contain the shift due to the imaginary part of the correlation function which is smaller than 5 cm^{-1} in all cases. Further notice that the VB 30 Ry results are slightly different from Ref. [24] where a 6.2 ps trajectory had been used.

PP	cut-off (Ry)	$L_{N\dots N}$ (Å)	$L_{N\dots O}$ (Å)	$\nu_{NH\dots N}$ (cm^{-1})	$\nu_{NH\dots O}$ (cm^{-1})	gap (cm^{-1})	$\Gamma_{N\dots N}$ (cm^{-1})	$\Gamma_{N\dots O}$ (cm^{-1})	$\Gamma_{N\dots N}^{AI}$ (cm^{-1})
VB	30	3.24	3.11	3235	3306	71	37	9	47
VB	40	3.09	3.14	3127	3306	179	41	13	37
TM	70	3.09	3.03	3132	3275	143	45	10	41
TM	100	3.10	3.09	3122	3276	154	54	8	55
GO	100	3.10	2.99	3183	3250	67	23	9	19
GO	140	3.09	3.05	3143	3293	150	15	5	13
Exp.	-	-	-	3185	3315	130	53	41	53

using the larger cut-off of 100 Ry does not necessarily give an improvement. Another point to mention is that Tab. I also shows that the correlation between average HB distance and average stretching frequency is not linear and in particular the fluctuations are sensitive to the used CPMD setup. The latter are also responsible for the linewidths which are compared in the right part of Tab. I. Also for this quantity the TM PP (70 Ry) performs reasonably well for the case of the $\nu_{N-H\dots N}$ transition. The FWHM of the $\nu_{N-H\dots O}$ transition is, however, considerably underestimated in all cases. Finally, we give the FWHM obtained by using the gap correlation function derived from the snapshot potentials. They are remarkably close the values calculated via the empirical correlation. This leads us to conclude that the quantitative difference between the two approaches is indeed merely a constant shift of the transition frequencies (cf. Fig. 6).

IV. SUMMARY

We have presented a QM/MM approach to the simulation of the intermolecular HB dynamics in solvated A:U pairs. On average the two HBs are almost linear and follow the empirical geometric relation of Limbach and coworkers between the HB lengths and the proton position. Further it was found that nonplanarity of the HBs is closely related to the compression due to bending motions of the C=O and NH groups. The trajectory mean of the dihedral angle formed by HB donors and acceptors is predicted as -19° . Exploring the empirical correlation between HB lengths and transition frequencies of the H-bonded protons we were able to simulate the IR spectrum in the region of the uracil NH and the adenine symmetric NH_2 stretching fundamental transition. Attempts to use transition frequencies derived from snapshot potentials gave considerably red-shifted transitions independent on the used pseudopotential and cut-off parameters. The difference between empirical and snapshot-derived frequency-distance correlation curves amounts to a shift of 450 cm^{-1} approximately independent on the HB distance. For the used empirical mapping the Troullier-Martins pseudopotential with a cut-off of 70 Ry gives the best agreement for the two fundamental transition. A multimode Brownian oscillator analysis of the gap correlation function yielded a spectrum of coupling strengths which is dominated by low-frequency vibrations, but contains contributions presumably from modes which modulate the two HBs in the range between $200\text{-}700\text{ cm}^{-1}$. While the width of the $\nu_{\text{NH}\cdots\text{N}}$ transition could be fairly well reproduced, the width of the $\nu_{\text{NH}\cdots\text{O}}$ transition is underestimated. However, one should be aware that our simulation does neither include contributions from other high-frequency modes nor combination bands which could give rise to an additional broadening of the experimental spectra.

Acknowledgments

We are indebted to Dr. S. Woutersen (Amsterdam) for the helpful discussion concerning the NH assignment and Dr. Yagi (Tokyo) for sharing his preliminary results on the anharmonic vibrational calculations. This work has been financially supported by the Deutsche Forschungsgemeinschaft (project Ku952/5-1).

-
- [1] G. A. Jeffrey. *An Introduction to Hydrogen bonding* (Oxford, New York, 1997).
- [2] K. Giese, M. Petković, H. Naundorf, and O. Kühn. *Phys. Rep.* **430**, 211 (2006).
- [3] E. T. J. Nibbering, J. Dreyer, O. Kühn, J. Bredenbeck, P. Hamm, and T. Elsaesser. In *Analysis and control of ultrafast photoinduced reactions* (edited by O. Kühn and L. Wöste) (Springer Verlag, Heidelberg, 2007), vol. 87 of *Springer Series in Chemical Physics*, p. 619.
- [4] C. Plützer, I. Hünig, K. Kleinermanns, E. Nir, and M. S. De Vries. *ChemPhysChem* **4**, 838 (2003).
- [5] G. M. Krishnan and O. Kühn. *Chem. Phys. Lett.* **435**, 132 (2007).
- [6] S. Woutersen and G. Cristalli. *J. Chem. Phys.* **121**(11), 5381 (2004).
- [7] K. Heyne, G. M. Krishnan, and O. Kühn. *J. Phys. Chem. B* **112**, 7909 (2008).
- [8] J. R. Dwyer, L. Szyc, E. T. J. Nibbering, and T. Elsaesser. *J. Phys. Chem. B* **112**(36), 11194 (2008).
- [9] P. Hobza and J. Sponer. *Chem. Rev.* **99**, 3247 (1999).
- [10] R. Ramírez, T. López-Ciudad, P. K. P, and D. Marx. *J. Chem. Phys.* **121**, 3973 (2004).
- [11] P. L. Silvestrelli, M. Bernasconi, and M. Parrinello. *Chem. Phys. Lett.* **277**, 478 (1997).
- [12] M. P. Gaijeot and M. Sprik. *J. Phys. Chem. B* **107**(38), 10344 (2003).
- [13] M. V. Vener and J. Sauer. *Phys. Chem. Chem. Phys.* **7**, 258 (2005).
- [14] A. Jezierska, J. J. Panek, A. Koll, and J. Mavri. *J. Chem. Phys.* **126**(20), 205101 (2007).
- [15] A. Jezierska, J. Panek, U. Borštnik, J. Mavri, and D. Janežič. *J. Phys. Chem. B* **111**(19), 5243 (2007).
- [16] A. Jezierska, J. J. Panek, and A. Koll. *ChemPhysChem* **9**, 839 (2008).
- [17] J. Stare, J. Panek, J. Eckert, J. Grdadolnik, J. Mavri, and D. Hadzi. *J. Phys. Chem. A* **112**(7), 1576 (2008).
- [18] H. Lin and D. G. Truhlar. *Theor. Chem. Acc.* **117**(2), 185 (Feb. 2007).
- [19] A. Laio, J. VandeVondele, and U. Rothlisberger. *J. Chem. Phys.* **116**(16), 6941 (2002).
- [20] P. K. Biswas and V. Gogonea. *J. Chem. Phys.* **123**(16), 164114 (2005).
- [21] R. Rousseau, V. Kleinschmidt, U. W. Schmitt, and D. Marx. *Angew. Chem. Int. Ed.* **43**, 4804 (2004).
- [22] G. Mathias and D. Marx. *Proc. Nat. Acad. Sci. (USA)* **104**(17), 6980 (2007).
- [23] M. Baer, G. Mathias, I.-F. W. Kuo, D. J. Tobias, C. J. Mundy, and D. Marx. *ChemPhysChem* **9**, 2703 (2008).

- [24] Y. Yan, G. M. Krishnan, and O. Kühn. Chem. Phys. Lett. **464**, 230 (2008).
- [25] S. Bratos, J.-C. Leicknam, S. Pommeret, and G. Gallot. J. Mol. Struct. **798**, 197 (2004).
- [26] CPMD. Copyright IBM Corp. 1990-2006, Copyright MPI für Festkörperforschung Stuttgart 1997-2001.
- [27] W. L. Jorgensen, D. S. Maxwell, and J. TiradoRives. J. Am. Chem. Soc. **118**, 11225 (1996).
- [28] D. van der Spoel, A. R. van Buuren, E. Apol, P. J. Meulenhoff, D. P. Tieleman, A. L. T. M. Sijbers, B. Hess, K. A. Feenstra, E. Lindahl, R. van Drunen, and H. J. C. Berendsen. *Gromacs User Manual version 3.1*. Nijenborgh 4, 9747 AG Groningen, The Netherlands. Internet: <http://www.gromacs.org> (2001).
- [29] D. Vanderbilt. Phys. Rev. B **41**(11), 7892 (Apr 1990).
- [30] N. Troullier and J. L. Martins. Phys. Rev. B **43**(3), 1993 (Jan 1991).
- [31] S. Goedecker, M. Teter, and J. Hutter. Phys. Rev. B **54**(3), 1703 (Jul 1996).
- [32] H.-H. Limbach, G. S. Denisov, and N. S. Golubev. In *Isotope Effects in Chemistry and Biology* (edited by A. Kohen and H.-H. Limbach) (Taylor and Francis, Boca Raton, 2006), chap. 7, p. 193.
- [33] M. Pietrzak, M. F. Shibl, M. Bröring, O. Kühn, and H.-H. Limbach. J. Am. Chem. Soc. **129**, 296 (2007).
- [34] H.-H. Limbach, M. Pietrzak, H. Benedict, P. M. Tolstoy, N. S. Golubev, and G. S. Denisov. J. Mol. Struct. **706**, 115 (2004).
- [35] A. Novak. Struct. Bonding **18**, 177 (1974).
- [36] W. Mikenda. J. Mol. Struct. **147**, 1 (1986).
- [37] S. Mukamel. *Principles of Nonlinear Optical Spectroscopy* (Oxford, New York, 1995).
- [38] C. P. Lawrence and J. L. Skinner. Proc. Nat. Acad. Sci. USA **102**, 6720 (2005).
- [39] C. C. Marston and G. G. Balint-Kurti. J. Chem. Phys. **91**, 3571 (1989).
- [40] P. Colarusso, K. Q. Zhang, B. J. Guo, and P. F. Bernath. Chem. Phys. Lett. **269**, 39 (1997).
- [41] Y. Kyogoku, S. Higuchi, and M. Tsuboi. Spectrochim. Acta A **23**, 969 (1967).
- [42] J. H. Miller and H. M. Sobell. J. Mol. Biol **24**, 345 (1967).
- [43] K. Yagi, S. Hirata, and K. Hirao. J. Chem. Phys. **127**, 034111 (2007).
- [44] K. Yagi. Private communication.
- [45] Note that the Gromacs/CPMD interface does not provide the capability to account for the QM charge density in the dipole calculation.